



Vibro-acoustic analysis of a steel railway bridge, with special regard to the potentials of active vibration damping

Tamás Mócsai, Krisztián Gulyás, Fülöp Augusztinovicz

Budapest University of Technology and Economics, Dept. of Telecommunications, Vibroacoustic Laboratory, H-1117 Budapest, Magyar Tudósok körútja 2., Hungary, e-mail: {mocsai, gulyas, fulop}@hit.bme.hu.

This paper reports on the details of an extensive vibro-acoustic analysis of a railway bridge of SNCB (Belgian National Railway) "line 40" at Liège. The work was carried out in the framework of integrated project InMAR (Intelligent Material for Active Noise Reduction). Vibrational and sound radiation control of steel railway bridges by means of integrated active damping devices is a new way of conscious environmental protection. In order to get a better insight into the vibrational and the sound radiation behavior of the bridge, a detailed measurement campaign was performed. For optimal placement of the active damping devices a complex numerical investigation of the bridge was carried out. This paper describes the details of the measurement campaign and presents the steps of validation of calculated results.

1 Introduction

Bridges, especially steel bridges are significant noise and vibration sources along railway lines. Passive solutions for noise and vibration mitigation have proven to be useful, but their economic efficiency is often dubious and the technical performance of such solutions shows some limitations, especially in the low frequency range .

The work to be performed is related to the EU project INMAR, aimed at conceiving, developing, testing and validating active noise and vibration control systems for specific applications related to bridges and tunnels. The characteristics of these active systems is to be optimised as a function of the parameters of the noise or vibration excitation source (frequency, amplitude, vehicle speed), and the systems are designed to provide a higher degree of performance than existing passive solutions.

In close cooperation with Micromega Dynamics, a Belgian SME partner in the project, a steel railway bridge with assumed large noise radiating areas across the river Ourthe in Liège, Belgium, has been selected as an appropriate testing object for detailed vibro-acoustic analyses. An active noise reduction solution has already been studied based on the hypothesis that the low frequency noise generated by the steel bridge during train passage is mainly due to local resonance of the steel lateral plates making the bridge. This solution works on the principle of increasing the structural damping of the lateral steel plates by using Active Damping Devices (ADD).

The aim of the works reported herein was to develop a vibro-acoustic model of the bridge [1][2] along a selected section (the shore span), which is sufficiently detailed to enable optimization of an active vibration damping system currently under development. In order to reach this goal, a number of measurements, calculations and various numerical and statistical approaches were developed

and applied. The measurements included operational vibration measurements, parallel operational vibration and noise measurements, and FRF measurements (for an experimental modal analysis test).

The investigations are still in progress. Here the conditions of the measurements are summarized and the evaluation of the measurement results reported. The applied numerical and statistical models and the obtained results are also discussed.

2 Measurements

The measurement tasks performed were the following: operational vibration measurements on the potential noise radiation surfaces of the bridge (presumably the side plates being the predominant radiators) for a number of train passbys; operational noise measurements (preferably parallel with vibration data recordings) in order to estimate the radiated noise and to verify subsequent vibro-acoustic simulations; and to perform an experimental modal analysis test on a selected part of the bridge, aimed at verifying the structural model of the bridge.

The preparation of the measurement series have taken place in Hungary. The measurement system consisted of a 16-channel data acquisition system Type LMS Test.Lab, equipped with standard industrial accelerometer sensors and a specially designed and manufactured low sensitivity, wide frequency range impact hammer. The system enables the analyst to perform multichannel measurements in the field, to check the recorded data immediately on site and to effectively analyze the recordings in the lab subsequently.



Figure 1: Measurement system and operators below the bridge

2.1 Vibrational measurement points

The measurement system has enabled us to record maximum 16 signals simultaneously. Considering both the measurement goals and the practical limitations (possibly minimal perturbation of pedestrian and road traffic and availability of cabling and safety personnel of SNCB), we have decided to perform the measurements along three sections of the bridge.

The selection of the points for the operational vibration measurements was decided on the basis of the preliminary FE model and earlier measurements of Micromega Dynamics. One reference point on the railhead and 15 points on the beams and stingers as well as in the middle of free steel plates were selected and measured.

Considering that the measurement time was very much limited, only 3×15 measuring points for the experimental modal analysis tests could be treated. The points were placed app. 60 cm apart along three horizontal lines (at the height of 1.9, 1 and app. 0.05 m as from the walking grid of the bridge interior, respectively), resulting in 6 points per parts between two main beams of the bridge section.

2.2 Microphone positions

Three points for noise measurements were selected. Point M1 was used to control downward radiation of the bridge, 1.6 m apart from the lower plates of the bridge. M2 was similarly at 1.6 m distance from the sidewall of the bridge, at 1.5 m height from the floor of the footbridge. Point M3 was selected at 15 m distance from the sidewall along a line normal to the axis of the bridge.

Note that the while the selection of M1 and M2 was rather obvious, the placing of M3 required to meet a number of contradicting conditions. On one hand, we wanted to measure the noise characteristics as far from the bridge as possible, in order to have representative information of the environmental disturbance of the bridge noise. On

the other hand, it was established the background noise of the urban environment was rather high even at late hours. Therefore, the road traffic was stopped. The most important limiting factor of the bridge to far-field microphone distance was however the fact that at higher distances an integral noise spectrum could only have been measured, including not only the radiation of the shore span but the riverbed span of the bridge too.

Considering that the riverbed span of the bridge is of a totally different structure and no vibration information whatsoever on that part of the bridge was available, this fact made the evaluation of the results rather difficult. It was assumed that the problem can be reduced by selecting a bridge-to-microphone distance which is com-measurable with the length of the shore span of the bridge.

3 Measurement results

3.1 Data preparation

Due to the high background noise levels, the noise radiation from the river-span bridge and the noise of the approaching coaches and loco itself, the clarity and reliability of the long time-signal takes/records were insufficient. The 30-80 sec long data records were truncated to represent only the most significant part of the time-signals when the train is on the bridge being investigated. The vibration signal of the rail measurement point was used to select and crop the appropriate time-section for further investigation.

3.2 Modal analysis

According to the measuring conditions described in Section 2.1, the measurement points were taken in three rows along the three selected sections of the bridge. One point in the upper row, another in the middle row on the sidewall and the rail were used as reference excitation points. These reference points were excited with impact hammer and the frequency responses measured by means of accelerometers (including the driving point FRF).

Based on the measurement data, three individual FRF sets were created and treated individually. Afterwards these three FRF sets were merged, in order to see, how this combination increases the reliability of the modal extraction.

The FRF set based on the reference point on the rail pointed strong resonant peaks around 20 Hz and above. The merged FRF set pointed only a few resonant modes, however each of them appeared in the previous FRF set.

3.2.1 Eigenfrequencies

The analysis of the assumed modes showed that the low-frequency modes are global of the entire bridge structure below 30 Hz. There are plate resonances (especially the 54-55 Hz mode is a local plate resonance) between 40 and 60 Hz. Above 70 Hz the applied measurement grid (the location of the points) seems to be more and more inappropriate to show the modeshapes correctly - the grid is not detailed enough to comply with the spatial sampling theorem.

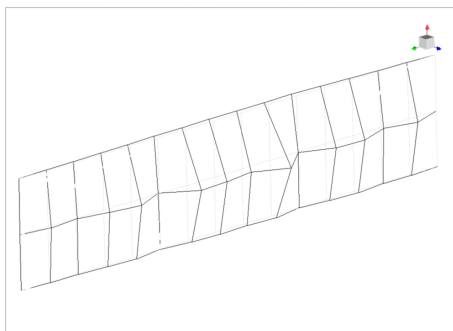


Figure 2: A typical local mode shape of the side plate at 55 Hz

3.3 Operational measurements

The aim of the operational measurements was to clarify the relationship between the vibration of the bridge and the radiated sound at near- and far-field. The narrow-band vibration and noise spectra were investigated together in order to determine the noise radiation mechanism of the selected bridge. In the first instance a strong relationship was assumed between the typical modeshapes and vibration of some surfaces of the bridge and the measured far-field noise.

3.3.1 Vibration and noise

Relevant peaks could be found in the near-field noise, the far-field noise and the vibration spectra at 24 Hz, 38 Hz, 42 Hz, 55 Hz, 80 Hz, 111 Hz. These peaks can be directly linked to the resonant mode frequencies.

Unfortunately, above 100 Hz the peaks in the vibration spectra can not be directly identified in the noise spectra. We also have to note that the low frequency (below 100 Hz) noise peaks associated with high vibration levels and vibration modes are not relevant in terms of the subjective audible noise levels, due to the characteristic of the human ear. A-weighting of the noise spectra reveals that the low-frequency noise peaks associated with the strong resonant modes below and around 100 Hz have irrelevant contribution to the A-weighted far-field noise levels.

Above 100 Hz high vibration levels occur from the side-plate and the stiffeners around 110 Hz, 130 Hz, 185 Hz, 200 Hz, 220 Hz, 246 Hz and 310 Hz. The bottom structure (plate and I beam) have strong vibrations around 168 Hz, 200 Hz, 315 Hz, 414 Hz that can be directly associated with peaks of the measured noise spectra under the bridge. Above 100 Hz the peaks of the far-field noise spectra stay in a 5 dB width band, being seemingly independent on the variations in vibration levels of the structure.

The near-field noise spectra shows a weak correlation with the higher than average vibration levels of the plate center at around 115 Hz, 160 Hz, 200 Hz, 234 Hz, 260 Hz, 300 Hz.

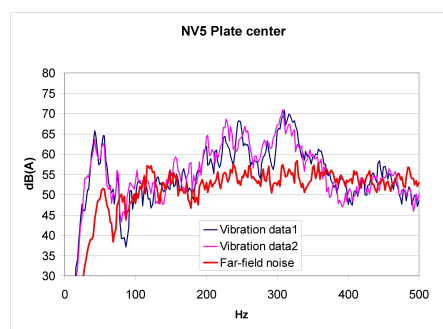


Figure 3: Spectrum of far-field noise and plate center vibration

3.3.2 FRF analysis

For the investigation of the vibration behavior of the ballasted bridge structure, various FRF curves between the railhead and the steel structure were compared. Based on the results we have to assume that the ballast track of the bridge has several nonlinear effect, and/or the dynamic behavior of the bridge structure itself can also be nonlinear. Different train types generate different loads to the rail and give rise to changed FRFs.

Below 100 Hz the difference between the related FRFs was not relevant, thus the structure could be assumed to be linear. The relatively small differences were thought to be some measurement errors caused by the differences of the excitation signals.

Above 100-200 Hz the differences between the FRFs were increasing. The related FRFs of the trains with light loads were similar, while trains with heavy loads caused relevant discrepancies.

4 Modeling

In order to get a better insight into the underlying phenomena of the selected and measured bridge, an extended

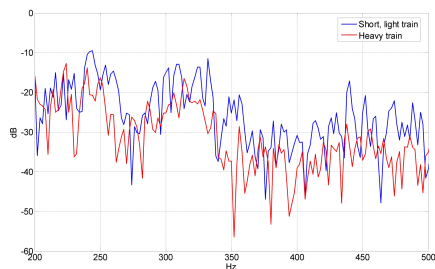


Figure 4: FRFs between the reference point on the rail-head and side plate center in case of different train loads above 200 Hz

numerical investigation was performed. Important part of this task is the development of the model; the numerical model should be as simple as possible in order to reduce the calculation time and the numerical complexity of the model related tasks. However the model should represent the main vibroacoustic properties of the modeled structure, e.g. neglecting any part of the investigated structure should be done very carefully.

4.1 Finite Element model

4.1.1 Description of the model

Due to the computational requirements of a detailed model, only a part of the bridge was modeled. A three-section (the whole bridge consists of 10 sections) finite element model of the bridge was developed by means of the software package MSC. Nastran 2004. The dimensions of the model are very close to the physical dimensions of the bridge. Even though a reasonable division of the finite element (FE) mesh was considered, in order to make the model as simple as possible, however the real dimensions of each part of the bridge had to be taken into account. Thus, this approximation was slightly limited by division of the FE mesh/grid. Further extensions and details of the bridge were examined. Finally the inclusion of the footbridge was neglected because it does not really affect the dynamic behavior of the overall structure. The size of the final model was 8889 nodes and 9247 elements.

The application of motion constraints for the modeling of the structural fixation of the bridge was also investigated. This tree-section model does not include the physical end terminals of the bridge. Modeling of a rigid fixation by means of applying a zero-motion constraint at the ends was also neglected. It is clear that the effects of truncation of the model are relevant; however inclusion of the entire bridge structure would lead to a computationally unmanageable and instable problem. However, we assumed that this model is sufficient for the investigation of the behavior of the side-plates, the main target of our

noise-related investigations.

4.1.2 Materials and element properties

The FE model of the bridge consists of 2D plate elements with appropriate material properties and thicknesses.

One of the most critical issue is the selection of the proper mechanical parameters of the ballast and the complex rail fixation system and the substructure (rail, railpad, sleeper, ballast) [3][4][5]. The effect of the modification of these parameters was investigated exhaustively. We assumed that some components are irrelevant in terms of the overall structural behavior of the bridge. Hence the modeling of the rail itself and the railpads was rejected. Further investigations showed that the effect of modifications of sleeper properties are also negligible.

4.1.3 Eigenvalue analysis

The eigenvalue analysis of the model pointed out hundreds of vibration modes because of the complex structure of the model. Below 100 Hz approximately 100 modes were detected. Most of these modes are the complex linear combinations of local resonances of some irrelevant structural details. The computed results showed good correlation with the modal analysis measurements around 20 Hz. At this frequency the model structure has a global mode shape. Mode shapes around 38 and 42 Hz were also found, in agreement with the measurements. The local resonances of side plates around 55 Hz were also detected.

The complex behavior and the high modal density below 100 Hz suggested that the modal approach of the structure is insufficient in this case. However, on the basis of the correlation between some computed and measured modeshapes it was assumed that by applying a proper model of the excitation the harmonic response analysis of the structure would point out a good approximation of the operational vibration behavior of the structure.

4.1.4 Harmonic response analysis

According to the statements and suggestions in section 4.1.3 two approaches were chosen for the validation of the model. These were the followings:

FRF validation A unit amplitude harmonic excitation force was applied on some model nodes (computed from 0 to 100 Hz with 2 Hz increment). The location of the excitation points was nearly at the same position as reference excitation points of the impact hammer in the modal analysis measurements. The computed response functions and vibration shapes were examined and compared to the measured ones.

Harmonic response analysis Using different configurations of the locations of excitation points along the sleeper elements of the model, the operational behavior of the structure was to be analyzed.

In the case of the rail excitation point investigations, the numerical results showed that the modeling efficiency of the rail fixation structure is problematic. Different parameters for the modeling of the ballast were also investigated. Modification of the damping factor in a wide range [6] has lead to relevant changes in the simulation results, however it did not give a better approximation of the behavior of the real bridge.

As a summary of the structural numerical analyses, one had to conclude that it is very difficult to build a numerical model which is accurate enough to predict the vibration behaviour of the investigated system, even if the frequency range of the investigations is limited to a relatively low frequency band. The difficulties stem partly from the physical and numerical size of the model, but the most important factor influencing the accuracy is the nonlinear and time-varying behaviour of the ballast. As mentioned above, time variance is a problem for the measurements too, hence it is not to be expected that good agreement between the measurements and numerical results can be obtained.

4.2 Contribution analysis

Due to the complex modal behaviour of the model and the associated analysis difficulties, a statistical approach was also attempted for the determination of the contribution from the main structural vibration sources. It was presumed that the far-field noise radiation is composed of two essential vibration sources: the bottom plate and the side plate of the investigated bridge section. The aim of this analysis is to determine, which one of these two predominates in the far-field noise radiation.

4.2.1 Radiation efficiency analysis

The calculation method is based on a number of rather stringent assumptions as follows: the vibration sources act as independent, hence uncorrelated, plate sources, radiating noise in form of plane waves in their immediate vicinity and their vibration is characterized by the spatial average of the surface velocity, resulting in the partial sound power contribution P (using $P = \int IA dA$):

$$P = \sigma \bar{v}^2 \rho_0 c A_{surf} \quad (1)$$

where σ means the so called radiation efficiency, $\rho_0 c$ is the specific impedance of the air, and A_{surf} stands for the total surface area of the assumed partial source. In

the case of the sideplate $A_{surf} \approx 90m^2$, in the case of the bottom part $A_{surf} \approx 150m^2$.

It is also assumed that the sound power is radiated in the form of a plane wave (though not necessarily normal to the radiating surface), therefore the radiated partial sound power can be determined from simple near-field sound pressure measurements:

$$10 \log \left(\frac{p_{near}}{p_0} \right)^2 = 10 \log \frac{\sigma \bar{v}^2 \rho_0 c A_{surf}}{P_0} \quad [dB]. \quad (2)$$

The radiation efficiency can then be calculated from the formula

$$\sigma = \left(\frac{p_{near}}{\bar{v}} \right)^2 \frac{P_0}{\rho_0^2 c A_{surf}}. \quad (3)$$

Eventually, assuming that the far-field microphone positions are far enough to enable one to take into account spherical sound propagation into the far field, the far-field sound pressure can be obtained from

$$p_{far} = P \frac{\rho_0 c}{2r^2 \pi}. \quad (4)$$

Using now Eq. 2 for the two assumed radiating surfaces where the near-field sound pressure spectra as measured in the microphone positions M1 and M2 are available, the radiation efficiencies of the partial sources can be calculated, and the far-field sound pressure can also be summed and compared to the sound spectra measured in the microphone position M3.

While the absolute value of the curves in Fig. 5 is most probably not entirely correct due to the inaccuracies of the spatial averaging (both in terms of surface vibrations and near-field acoustic measurements), the increasing tendency of the functions is realistic, thus the bottom plate seems to be a better radiator than the side plate.

The relative contribution of the two plates and their energy sum is given on Fig. 6, as compared to the measured far-field sound spectrum. The measured and the calculated spectra do differ by app. 10 dB, but the trends and spectrum shapes agree quite well.

By taking into account that using averaged velocity distribution of the bottom plate and I-beam, the velocity levels of the bottom structure are higher than the levels of the sideplate around 100 Hz and above 400 Hz. The calculated radiation efficiency and the assumed radiating surface area of the bottom part is also higher. Thus one can draw the qualitative conclusion that the bottom plate most probably plays a more important role in the far-field radiation than the side plate.

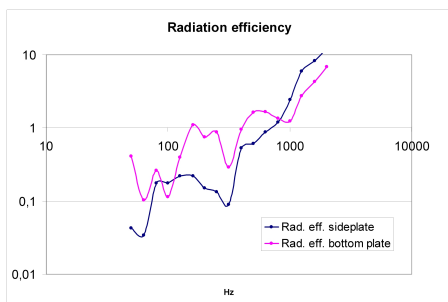


Figure 5: Radiation efficiency

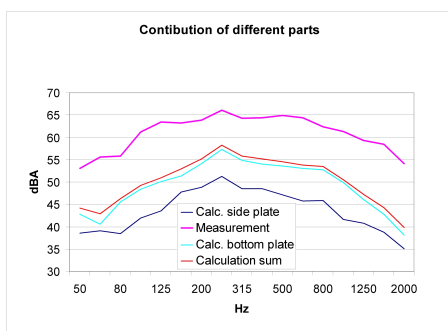


Figure 6: Contribution of parts

5 Conclusions

It was established that at low frequencies, i.e. below 80 Hz or so, the far-field noise radiation is characterized by a few narrow band components (38 Hz, 42 Hz, 55 Hz, 74 Hz and 77 Hz), which can obviously be attributed to the lightly damped resonant vibration of the side plates of the investigated bridge section. Considering that most of these mode shapes are not global but local modes of the plates between the main beams and stingers, they can most likely be damped out effectively by using the ASAC system, currently in development. The placement of the damping element can be optimized by using the aforementioned mode shapes, and in case of necessity a relatively simple hybrid FE model can also be developed and run for an effective optimization.

The main stumbling block of the modeling process is that the modal approach is a viable option in a rather low frequency range only. The frequency analysis of the far-field noise has revealed, however, that the low frequency components are not predominant in the far-field noise. Instead, the A-weighted sound spectrum measured at 15 m distance from the bridge consists of its strongest components above 100 Hz. Local maxima of the noise spectrum in this frequency range cannot be attributed to distinct normal modes of the vibrations, due to the high modal density of both the experimental and the numerical modal analysis. At the same time, one has to stress here that the limitations of the modal model approach does not neces-

sarily mean that an active vibration control system which is designed to damp out the resonant peaks of lightly damped systems, can not work effectively at higher frequencies too, up to 500 Hz or even higher.

We had to establish that our attempts to develop a reasonably accurate FRF-based calculation model of the bridge structure for a higher frequency band has failed. The main reason for it is probably twofold. For one, modeling of the ballast in form of mass and damping elements such as usual in the structural FE calculations, does probably not describe the behavior of the time- and load-dependent, and most likely non-linear transmission behavior of the ballasted substructure. On the other hand, the rolling motion and the time variant, moving load of the rail vehicles would certainly have required a more complex modelling of the excitation, which is well beyond the scope of this study.

It seems that the very simple statistical contribution analysis has revealed an important feature of the testing object, namely that the bottom plate is a more important radiator for the far-field than the side plate. If this is really the case, it can explain, why not much more normal modes of the freely vibrating side plate can be found back in the far-field noise. Unlike the side plates, the bottom plate certainly vibrates in forced mode, because most eigenmodes or resonant vibrations are probably damped out by the heavy and highly damping ballast. This difference probably deteriorates the potential usefulness of the ANC system, planned to be based on the application of the ADD elements.

References

- [1] M.H.A. Janssens, 'A calculation model for the noise from steel railway bridges', *Journ. Sound Vib.*, Vol. 193, No. 1. pp. 295-304. (1996)
- [2] J.G. Walker, 'An investigation of noise from trains on bridges', *Journ. Sound Vib.*, Vol. 193, No.1. pp. 307-314. (1996)
- [3] A.P. de Man, 'A survey of dynamic railway track properties and their quality', . PhD Thesis, Technische Universiteit Delft, 2002.
- [4] T.X. Wu, 'Theoretical investigations of wheel/rail non-linear interaction due to roughness excitation', ISVR Technical memorandum, 2000
- [5] F. Augusztinovicz, 'Vibro-acoustic design method of a tram track on a steel road bridge', Paper to be published in *Journ. Sound Vib*
- [6] W.M. Zhai, 'Modelling and experiment of railway-ballast vibrations', *Journ. Sound Vib*, 2003